

BIOSYNTHESIS OF CUO, AND ZNO NANOPARTICLES USING LACTOBACILLUS PLANTARUM BACTERIA FOR ANTICANCER ACTIVITY

Jawad N. K. Makassees 1,

Ali A. Fayyadh 2,

Ali K. Hattab 3

1 Ministry of Education, General Directorate of Wasit Education, Wasit, Iraq.

2 Ministry of Education, General Directorate of Wasit Education, Wasit, Iraq.

3 Department of Physics, College of Science, University of Wasit, Wasit, Iraq.

*Corresponding Author: jalmaksusse@uowasit.edu.iq, alia224@uowasit.edu.iq,
ahatab@uowasit.edu.iq

Abstract:

Biosynthesis of copper oxide and zinc oxide nanoparticles by sustainable and environmentally friendly procedure using *Lactobacillus plantarum* bacteria as a reducing and capping agents. The biosynthesized nanoparticles were characterized using different techniques. XRD results demonstrated that the synthesized CuO crystals possessed a tenorite monoclinic phase with an average crystallite dimension of 24.78 nm, while ZnO formed hexagonal wurtzite crystals of 27.41 nm length. SEM analysis showed that CuO nanoparticles existed as quasi-spherical shapes while ZnO nanoparticles displayed hexagonal rod-like structures that matched their crystal arrangements. The EDS analysis showed both nanoparticles contained high-purity elements while they harbored only minimal bacterial remnants. The MTT assay was utilized to evaluate the anticancer activity of CuO/ ZnO nanoparticles against K562 erythroleukemic cells with normal human fetal fibroblast (HFF) cells serving as controls. The biosynthesis of metal oxide nanoparticles showed potential cancer therapy options for erythroleukemic conditions where CuO nanoparticles proved superior anticancer efficacy compared to ZnO nanoparticles. The CuO nanoparticles exhibited good cytotoxicity against cancer K562 cells with an IC₅₀ value of 135.46 µg/ml, whereas, ZnO nanoparticles exhibited a moderate activity showing an IC₅₀ of 438.23 µg/ml. Notably, CuO/ZnO nanoparticles displayed selective cytotoxicity against cancer K562 cells and minimal cytotoxicity against normal HFF cells, where the viability rates stayed above 65% even when high concentrations were applied. This selective targeting ability is credited to the variability in the functionality of a membrane, metabolic rates, and antioxidant defense mechanisms between cancer and normal cells, plus the formation of protein layers of corona on the surface of the nanoparticle.

Keywords: Biosynthesis, nanoparticles, crystallite, cytotoxicity, anticancer.



Introduction

Cancer represents one of the key reasons for death throughout the world and traditional chemotherapy approaches are regularly accompanied by a restricted impact due to the cumulative toxicity of the medicine, drug resistance, and poor specificity [1]. As a result, there is a rapid increase in the development of new therapeutic methods with higher efficacy and fewer adverse effects. Cancer therapy has emerged to be one of the greatest fields of applications of nanotechnology on account of the high surface- to- volume ratio, tunable size, and surface functionalization properties of metal oxide nanoparticles, which have increasing attention [2]. Cu-oxide (CuO) and Zn-oxide (ZnO) have demonstrated a strong potential to fight against cancer. They use several mechanisms whereby they produce reactive oxygen species (ROS), apoptotic induction, inhibits the cell cycle and causes DNA damage on cancer cells. Plagued by their promise, the former legacy physical and chemical methods of producing such nanoparticles tend to be supported by dangerous chemicals, drain a lot of energy, and can produce toxic waste. These problems are a matter of grave concern in terms of their environmental impact and the safety they have for medical use [3,4]. Recently, the biosynthesis or green synthesis of nanoparticles via the use of microorganisms has become popular because it is an environmentally-friendly, economical, and biocompatible option [5]. The biosynthesis technique uses the organic compounds found in microorganisms as reducing and stabilizing assays, and this eliminates the need to use toxic chemicals and complicated procedures. *Lactic acid* bacteria especially the *Lactobacillus* genus, stand out among diverse microorganisms is a factor in the production of nanoparticles due to their strong virulent enzymatic machinery and metabolic abilities, respectively [6]. *L. plantarum* is a gram positive, facultative anaerobic bacterium which is commonly found in various fermented foods and also is commonly present in our gut. It has a diverse set of enzymes that can cause the conversion of metal ions to nanoparticles [7]. This organism generates extracellular enzymes, proteins, and other metabolite that can be used as natural reducing and stabilizing assays. Hence, the formed nanoparticles become not only stable but also more biocompatible, which makes *L. plantarum* an appealing candidate for the green nanoparticle synthesis [8]. Despite the fact that many of the previous investigations have sought to advance our knowledge in relation to the biosynthesis of metal oxide nanoparticles utilizing diverse microorganisms, the efficiency of *L. plantarum* in the synthesis of CuO and ZnO nanoparticles and their anticancer applications have been relatively uncovered. Therefore, this study seeks to determine biosynthesis of CuO and ZnO nanoparticles with the use of *L. plantarum* and determine the cytotoxicity toward K562 erythroleukemic with normal human fetal fibroblast (HFF) cells as controls. The study contributes to the growing body of knowledge on green synthesis of nanoparticles and metal oxide promising potential uses in cancer treatment, highlighting the importance of sustainable and biocompatible approaches in nanomedicine.



Material and Methods**Material**

Copper sulfate pentahydrate ($\text{CuSO}_4 \cdot 5\text{H}_2\text{O}$) and zinc sulfate heptahydrate ($\text{ZnSO}_4 \cdot 7\text{H}_2\text{O}$) were obtained from Sigma-Aldrich (St. Louis, MO, USA). De Man, Rogosa, and Sharpe (MRS) broth and agar from HiMedia Laboratories (Mumbai, India). RPMI-1640 medium, Dulbecco's Modified Eagle Medium (DMEM), fetal bovine serum (FBS). The cell culture experiments were carried out using a penicillin/streptomycin solution, L-glutamine, and trypsin-EDTA, which were acquired at Gibco (Thermo Fisher Scientific, Waltham, MA, USA), whereas MTT and DMSO were obtained at Merck (Darmstadt). PBS tablets were obtained at Oxoid Ltd. (Hampshire, UK). All experiments were done using ultrapure water ($18.2 \text{ M}\Omega \cdot \text{cm}$).

Methods**Bacterial Strain and Culture Conditions**

Lactobacillus plantarum was originally isolated from 25 clinical samples using the routine isolation procedure employed by our lab. Bacterial isolate was identified using the standard techniques of microbiology, that is, Gram staining, colony morphology, and biochemical identification by catalase and oxidase, and sugar fermentation test. The established *L. plantarum* strain was retained on MRS agar and stored as glycerol stocks at -80°C . To obtain periodic growth, a single colony of *L. plantarum* was put into an MRS broth, then incubated for 24 h at (37°C) in the anaerobic atmosphere in an anaerobic jar with AnaeroGen sachets (Oxoid, UK). The late exponential phase ($\text{OD}_{600} \approx 1.8$). The bacterial culture was centrifuged at 4°C ($6000 \times g$ in 15 min).

Biosynthesis CuO and ZnO nanoparticles

Preparation of cell-free extract: the pellet of the bacteria was washed twice using sterile PBS (pH 7.4) and then re-suspended in PBS to give a final concentration of approximately 10^9 CFU/mL. The bacterial suspension was then sonicated (Sonics Vibra-Cell VCX 130, USA) at 40% amplitude with 30 s pulses and 30 s intervals for 10 min on ice. The cell debris was stripped by centrifuging the aliquot of the sonicated mixture at $12,000 \times g$ and 4°C for 20 min. Obtained supernatant was filtered with the help of $0.22 \mu\text{m}$ Millipore (USA) membrane filter and was utilized as cell-free extract in the production of nanoparticles.

Synthesis of CuO nanoparticles: 10 mL of cell-free extract and later neutralizing 90 mL of 1 mM copper sulfate solution. Incubation was performed for 48h at the reaction mixture in 0.5mL microtubes at 30°C with constant stirring at 150 rpm. The change of color from light blue to brownish-black revealed the development of CuO nanoparticles. The centrifugation of nanoparticles at 10000 rpm for 20 min using ultrapure water removed unreacted salts and bacterial proteins from them. The dried nanoparticles were then purified which were dried again for 24 h at 60°C in a hot air oven.

Synthesis of ZnO nanoparticles: 10 ml of the culture was combined with 90 mL of 1 mM zinc sulfate solution. The mixture was incubated for 48 h at 30°C with continuous stirring at 150



rpm. The process of formation of ZnO nanoparticles was evident from the color change from colorless to white. The nanoparticles were harvested by centrifugation (10,000 rpm, 20 min) and washed extensively in ultrapure water. The obtained ZnO nanoparticles were dried at 60°C for 24 h.

Cell Culture

Human erythroleukemic K562 cell line and normal human fibroblast (HFF) cells were purchased as cryopreserved vials in American Type Culture Collection “ATCC, Manassas, VA, USA”. RPMI-1640 Medium supplemented with 10 % FBS, 2 mM L-glutamine and 1 % penicillin-streptomycin were used to cultures K562 cells. Culturing of HFF cells was performed in DMEM 10% FBS, 2 mM L-glutamine; 1% penicillin-streptomycin. The culturing of both cell lines was done in a coefficient atmosphere of 5% CO₂ and at a temperature of 37 °C. At 80 to 90 % confluence, the cells were subcultured and culture medium was changed after every 48 hrs.

Cytotoxicity Assessment by MTT Assay

Cytotoxic effects of biosynthesized CuO and ZnO nanoparticles were determined by MTT (tetrazolium violet) colorimetric assay. For the K562 cells, a seeding weight of 1×10^4 cells per well was used in the 96-well plates, and for the HFF cells, a seeding weight of 5×10^3 cells/well was used. The cells were subsequently exposed to different concentrations (0; 25; 50; 100;200; 400;800) µg/mL of CuO or ZnO nanoparticles suspended in respective culture media after 24 hrs of incubation. The nanoparticle suspensions were prepared from stock solutions fresh just before use, sonicated for 15 min to avoid aggregation, and sterilized using 0.22 µm glass filters before use. After incubation for 48 hrs, 20. ul of MTT solution (5mg/ml) in PBS was then added to each well and incubated at 37 °C for 4 hrs. Then, for adherent HFF cells, the medium was removed with care, followed by dissolving the formed formazan crystals in 150 µL of DMSO. The centrifugation of the plates with a suspension of K562 cells was done at 1,500 rpm during 5 min, the supernatant was carefully removed and the formazan crystals were dissolved in 150 µL of DMSO. Absorbance was displayed at 570 nm with a reference at 630 nm with the micro plate reader (BioTek Synergy H1; USA). A cell viability was determined with the help of the following equation:

$$Cell\ viability = \left\{ \left[\frac{Absorbance\ of\ treated\ cells}{Absorbance\ of\ control\ cells} \right] \times 100\ \% \right\} \dots \dots \dots 1$$

The software GraphPad Prism (version 8.0, GraphPad Software Inc., San Diego, CA, USA) calculated the half maximal inhibitory concentration (IC 50) against the log of nanoparticle concentration.

Characterization

The crystalline structure determination was achieved through X-ray diffraction (XRD) utilizing a Bruker D8 advanced diffractometer. Operating parameters were monochromated Cu Kα



radiation ($\lambda=1.54060 \text{ \AA}$) at 40 mA and 50 kV. Diffraction patterns were automatically recorded within the 2θ range of $20\text{-}90^\circ$ intervals with high-resolution data acquisition parameters (0.01° step size and 1.5 s per step). Surface topology and nanostructural features were observed with the Hitachi SU8220 field emission scanning electron microscope, which was operated with an acceleration voltage of 20 kV. An energy-dispersive X-ray spectroscopy with an EDAX detector system quantitative elemental analysis was also carried out.

Result and discussion

The crystalline structure of CuO and ZnO nanoparticles was analyzed by X-ray diffraction (XRD). X-ray diffraction functions based on Bragg's law that establishes a relation between interplanar spacing and diffraction angle.

$$n\lambda = 2d \sin \theta \dots\dots\dots 2$$

The X-ray diffraction pattern depends on four main elements which include the diffraction order (n) and X-ray wavelength (λ) as well as the crystal lattice plane spacing (d) and X-ray beam incident angle (θ) [9]. The relation functions as a fundamental basis for crystal structure discovery in crystalline substances. The crystallite size has been estimated by using the Debye-Scherrer equation:

$$D = 0.9\lambda/\beta\cos\theta \dots\dots\dots 3$$

D is the crystallite size, and λ is the wavelength of the X-ray, β is full-width at half-intensity (FWHM) of the diffraction peak, and θ is the Bragg angle [10]. The X-ray diffraction patterns confirm successful biosynthesis of crystalline ZnO and CuO nanoparticles with *L. plantarum* as the biological mediator. The clearly defined diffraction patterns suggest that the bacterial synthesis route would give rise to high-quality nanocrystals with specific phase compositions which are appropriate for use in biomedical applications. The XRD patterns of the CuO nanoparticles shown in the figure (1) exhibit characteristic peaks at the 2θ values of 35.57° , 38.76° , and 48.79° which align with the monoclinic tenorite phase (entry COD: 96-901-6327). Bacterial synthesis of pure crystalline CuO shows the efficacy of *L. plantarum* to enable the reduction and oxidation processes that are needed to form CuO as reported by [6].

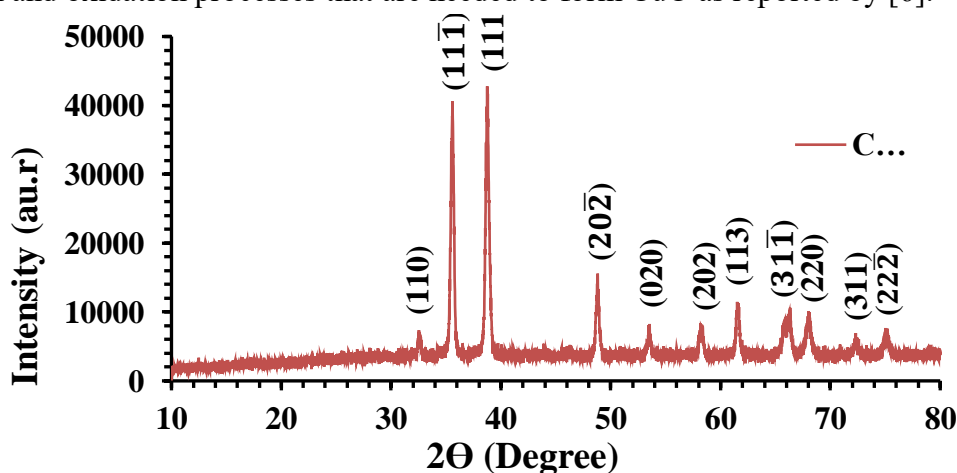


Fig. (1): XRD pattern of copper oxide (CuO) NPs.

Average size 24.78 nm crystallites with fairly uniform size distribution over different crystallographic orientations present controlled biosynthesis conditions. This size range is especially significant in terms of anticancer applications as CuO nanoparticles operating in this size range have been shown to actively cause selective cytotoxicity with cancer cells through reactive oxygen species (ROS) generation and DNA damage [2,11]. The diffraction peaks of characteristic nature in the biosynthesized ZnO nanoparticles XRD patterns shown in the figure (2) correspond to 2θ values of 31.915° , 34.576° and 36.395° which are indexed to the (100), (002), and (101) planes of “hexagonal wurtzite” structure (COD entry: 96-900-8878). The close resemblance of d-spacing values of experimental samples and the standard references validates the formation of pure-phase ZnO free of such contaminants and bacterial residues that would affect the crystal lattice. These results correlate with the results of previous studies on biosynthesized ZnO nanoparticles [8]. The average crystallite size of 27.41 nm is characterized as being within the desirable range of natural interactions, since the nanoparticles of 20-30 nm have been shown in literature to exhibit improved uptake in the cells and anticancer efficacy [12]. The minor preferential growth in terms of (002) direction (32.15 nm) should have some effect on the particle morphology and therefore on the biological activity of the particles, an observation previously reported by [13]. The successful crystalline metal oxide nanoparticle formation using *L. plantarum*-mediated synthesis marks on a major advancement in the green nanomaterial fabrication. The bacterial synthesis presumably requires extra cellular enzymes and metabolites which are able to mediate the reduction of metal ions and then onward oxidation of metal ions to form stable metal oxide nano structures [14].

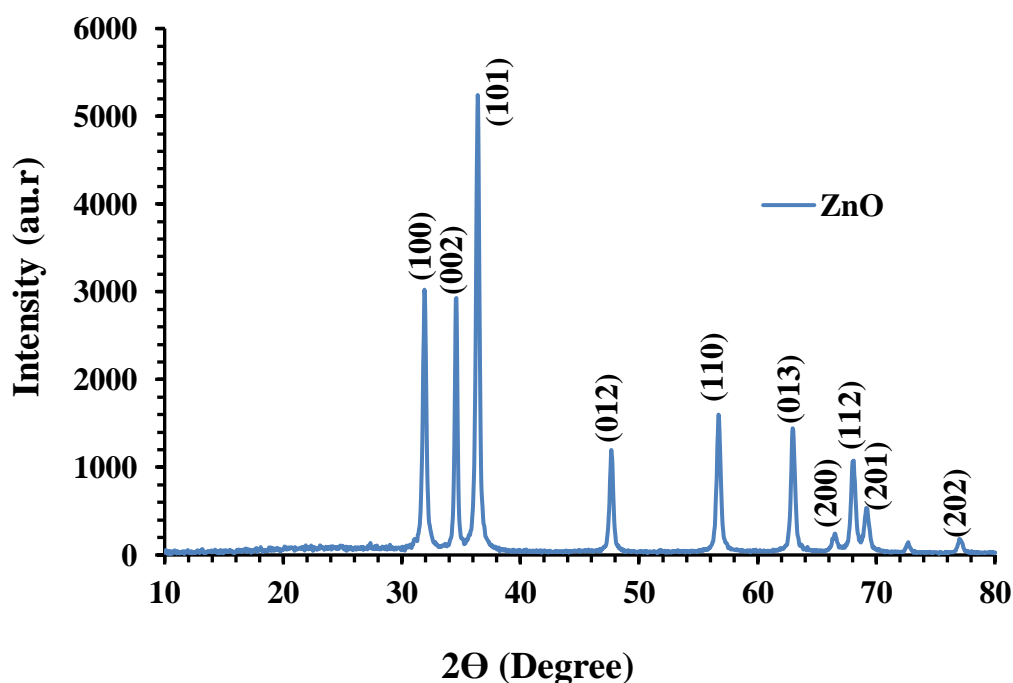


Fig. (2): XRD pattern of zinc oxide (ZnO) NPs.



The fact that the narrow size distribution and high crystallinity were observed both in CuO and ZnO samples indicates that bacterial synthesis is able to give control over nucleation and growth process possibly without hazardous chemicals, traditionally required in the conventional synthesis approach [15]. XRD analysis is an important key in deciphering the structural characteristics of biosynthesized nanoparticles, and the nature of these characteristics in relation to their anticancer potential. The crystallite sizes, which vary between 24–27 nm, are adequate for uptake by cells, if they have an appropriate surface area for biological interactions. Their high crystallinity may also favor the production of ROS, that major mechanism in which metal oxide nanoparticles kill cancer cells [16,17]. Furthermore, the purity of the phases investigated through XRD confirms that the anticancer activity documented can surely be attributed to ZnO and CuO nanoparticles and not because of the presence of unwanted phases or impurities. Because of the biogenic synthesis of these nanoparticles, they may also provide enhanced biocompatibility than the chemically synthesized ones, which might reduce the chance of toxicity to healthy cells [18,19]. Overall, XRD offers important structural confirmation which supports further use of such nanoparticles in biologic testing and allows for defining a direct relationship between their crystal structure and anticancer activity.

The SEM micrographs of biosynthesized CuO nanoparticles figure 3 (a) show quasi-spherical morphology with moderate agglomeration. At both magnifications, the particles show relatively uniform size distribution with diameters, that is, approximately 20-30 nm, which is well correlated with the XRD-derived crystallite size of 24.78 nm. The minimal agglomeration observed can be explained by high surface energy of nanoparticles and possible cross-linking by bacterial biomolecules serving effectively as capping agents [11]. The surface texture exhibits moderate roughness with interconnected particulates which suggests mechanism of nucleation and growth utilizing bacterial proteins and metabolites to mediate it. This morphology is favorable for anticancer applications as it has high surface area-to-surface ratio for better cellular interplay and drug loading possibility [20].

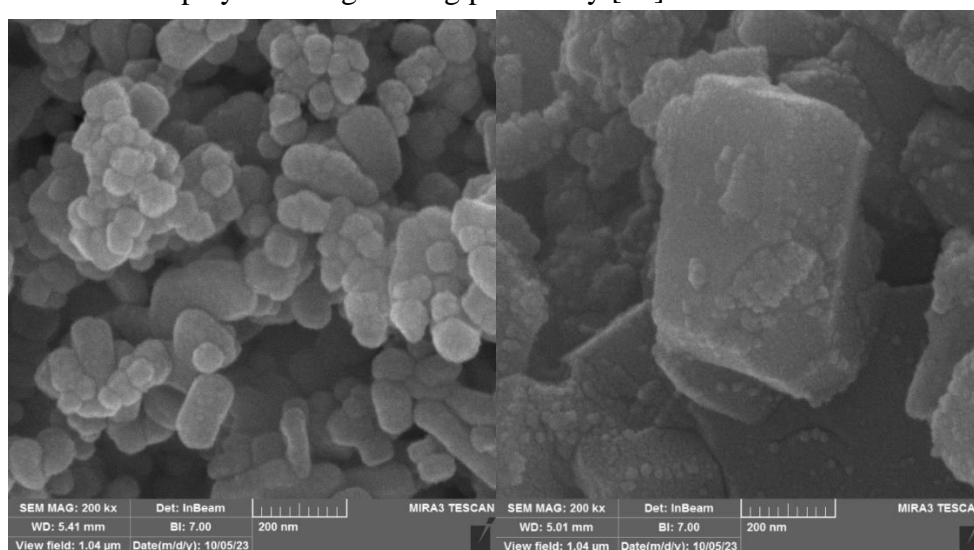


Fig. (3): SEM surface morphology of CuO (a-left) and ZnO (b-left) nanoparticles.



The ZnO nanoparticles figure 3 (b) exhibit a more pronounced morphology consisting of hexagonal/rod-like structures with facets, associated with the wurtzite crystal structure identified by the XRD. The particles seem to be a little bigger than CuO nanoparticles, their size being somewhere around 25-35 nm, which correspond to the calculated by the XRD average crystallite size of 27.41 nm. The particles are displayed with crisp boundaries and defined shapes unlike CuO suggesting various growth mechanisms in *L. plantarum* mediated biosynthesis. The observed morphology is of particular value in anticancer applications due to the reported increased photocatalytic properties and ROS generation ability of hexagonal ZnO nanostructures, directly correlating with the cytotoxicity towards cancer cells [12,16].

The EDS spectrum figure 4 of biologically synthesized CuO nanoparticles attest to the successful preparation of a copper oxide with low impurities. Quantitative analysis indicates a composition that is 70.26 wt% Cu and 20.24 wt% O, which approximates the theoretical stoichiometric in a CuO structure. The carbon 9.51 wt% can be attributed to organic residues of the *L. plantarum* bacterial synthesis process and in particular extracellular proteins and metabolites that possibly act as capping and stabilizing agent during nanoparticle formation [6]. The atomic percentage distribution (34.97% Cu and 40.00% O) further favors the phase of the oxide as opposed to elemental copper, with the excessive oxygen above stoichiometric level indicating possible surface oxidation or, adsorbed hydroxyl groups typical for biogenic nanoparticles [7]. The strong characteristic at 8.09 keV (Cu K α) and 0.54 keV (O K α) with the probability 100 % identification confirms the primary elemental composition with no detectable metallic impurities indicating high purity of biosynthesized CuO nanoparticles. This elemental purity is necessary for biomedical use especially; anticancer therapies where the inclusion of unintended metals could create a confounding toxicity [2].

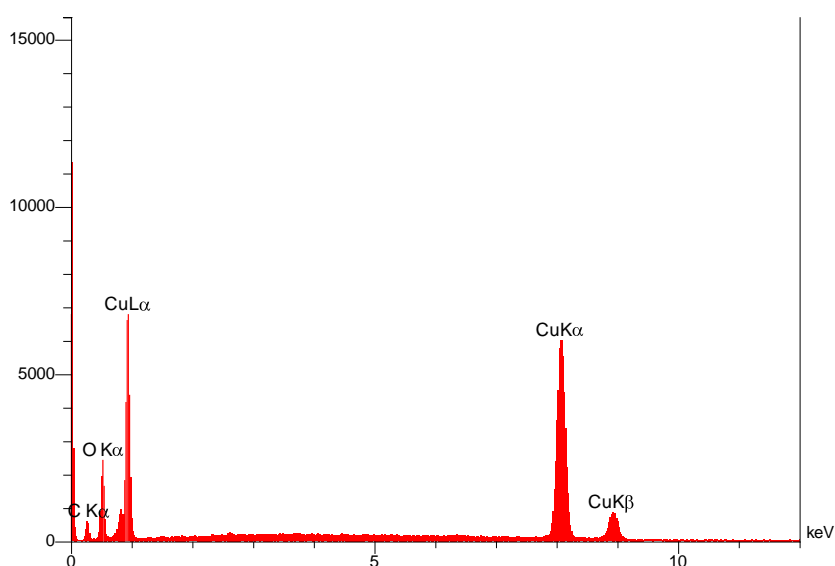


Fig. (4): EDS spectrum of CuO nanoparticles.



In case of ZnO nanoparticles, EDS spectrum figure 5 also confirms successful biosynthesis with Zn and O as the major elements. The quantitative results give; 55.51wt% Zn and 40.73 wt% O, which is close to the stoichiometric composition for ZnO. The 22.90% Zn and 68.65% O atomic percentage ratio suggests oxygen-rich surfaces, a typical phenomenon associated with biosynthesized ZnO nanoparticles which can increase their potential to generate reactive oxygen species (ROS) [17]. The lower carbon content (3.76 wt%) of ZnO *L. plantarum* compared to CuO nanoparticles indicates varied interaction mechanism of *L. plantarum* metabolites and zinc ions during biosynthesis [8]. The automatic identification results indicate strong peaks of 8.67 keV (Zn K α) and 0.51 keV (O K α). The detection of trace signals of Na, Ne, Zr, Re and Ra, at very low probability levels could be contributed to by background noise or minimal contaminants from bacterial culture medium which is a common trend observed in green synthesis methods [14].

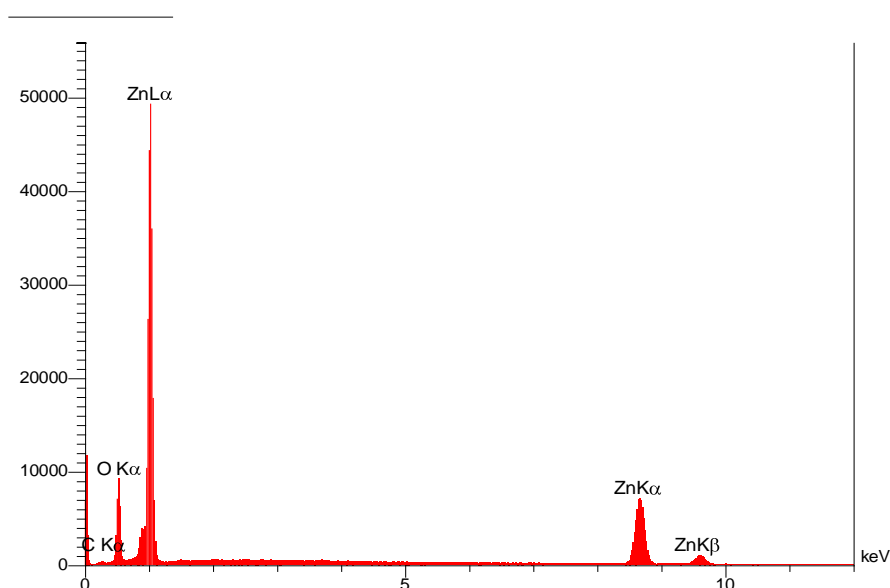


Fig. (5): EDS spectrum of ZnO nanoparticles.

The elemental composition and morphological characters of biosynthesized CuO and ZnO nanoparticles play a key part in determining their anticancer potency. The EDS analysis confirmed high purity and near-stoichiometric ratios, showing that the cytotoxicities seen could indeed be ascribed reliably to the actual metal oxides and not its contaminants. The presence of carbon in both samples suggests the capping by bacterial biomolecules not only ensures that the surface is biocompatible but it may have functional groups for targeted drug delivery[21]. Of two nanoparticle types, the particle sizes (20–35 nm) lie in an optimal range that allows cellular uptake and endocytosis (an important step necessary for anticancer activity to be effective). Their unique morphologies, quasi-spherical CuO and rod-like or hexagonal ZnO, may have different effects on cancer cells and can produce reactive oxygen species (ROS) from complementary mechanisms. Interestingly the moderate agglomeration noted can help

maintain releases of toxic metal ions in the acidic tumor environment thus prolonging its therapeutic effect [22]. These structural and compositional properties taken together support a powerful physicochemical rationale for the biological testing of these nanoparticles and may inform their use in targeted and efficient cancer therapy [23].

MTT Assay for Cytotoxicity of CuO and ZnO Nanoparticles

The cytotoxic effects of biosynthesized CuO and ZnO nanoparticles were evaluated in the human erythroleukemic cell line (K562) and human fetal fibroblast (HFF) cell line through the MTT assay. A dose-responsive response was evidenced in both cell types after an 48h of exposition at the physiological temperature (37°C). As demonstrated in Figure 6, CuO NPs induced significant dose-dependent toxicity in K562 cells. Cell viability decreased as the CuO NPs' concentration rose from 25 to 800 µg/mL, from $64.5 \pm 11.4\%$ to $39.5 \pm 12.5\%$; IC₅₀ was recorded 135.46 Strikingly, consequences of the normal HFF cell exposure to these nanoparticles showed markedly decreased cytotoxicity, with HFF viability staying within the range of $86.5 \pm 6.4\%$ to $72.6 \pm 6.6\%$ at the tested concentration range (Table 1). The observation of different cytotoxic effects on cancer from normal cells reinforce the idea that CuO NPs have a potential anticancer mechanism particularly that is needed for the clinical usage.

Table (1): Cytotoxicity effect of CuO and ZnO NPs on K562 and HFF cells after 48 hrs incubation at 37 °C.

Concentration µg mL ⁻¹	Mean Viability (%) ± SD			
	K 562 CuO NPs	HFF	K562 ZnO NPs	HFF
800	39.5± 12.476	72.573± 6.632	51.75 ± 41.580	71.870 ±33.630
400	40.05 ± 19.568	71.448± 5.715	46.45 ±10.5	73.488 ±30.554
200	46.45 ± 6.184	81.082±9.105	34.75 ± 7.932	65.260 ±8.640
100	46.45 ± 11.264	85.302 ± 2.753	41.95 ± 24.730	70.253 ±25.104
50	46.55 ± 11.265	86.990 ± 5.439	45.25± 23.837	73.347 ±9.358
25	64.5± 11.445	86.497 ± 6.350	97.25 ± 40.037	93.178±10.045
0	100± 29.518	100 ± 24.090	100 ±29.518	100 ±24.090

ZnO NPs also exhibited concentration-dependent cytotoxicity with differing potency and response profiles. As it is seen in Figure 7, K562 cell viability fell from $97.3 \pm 40.0\%$ at 25 µg/mL to $34.8 \pm 7.9\%$ at 200 µg/mL after exposure to ZnO NPs At high concentrations (400-800 µg/mL), cytotoxic effects plateaued rather than escalating, possibly reflecting saturation or aggregation limiting bioavailability.



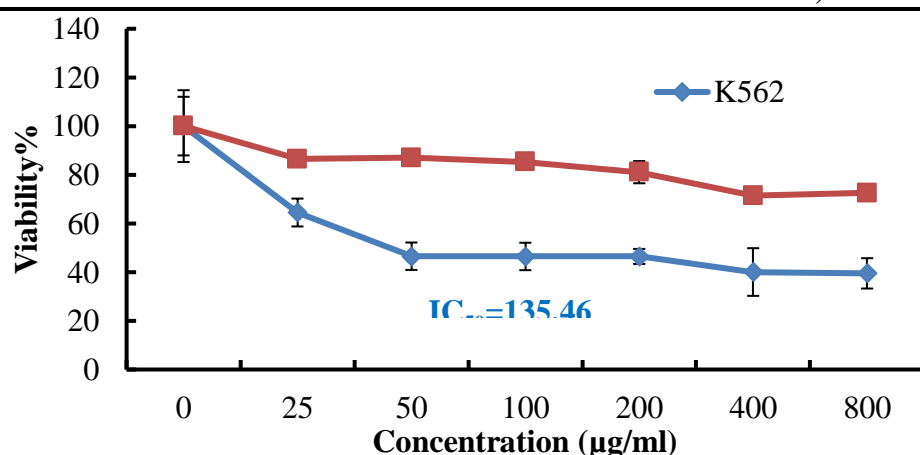


Fig. (6): Cytotoxic effect of CuO NPs on K562 and HFF cells after 48 hrs incubation at 37°C. The obtained IC_{50} value for ZnO NPs (438.23) $\mu\text{g/mL}$ implies that the cytotoxicity of ZnO NPs is significantly milder compared to that reported for CuO NPs. ZnO NPs, similar to CuO NPs, exhibited low toxicity towards normal HFF cells with cellular viability ranging in a narrow range of $93.2 \pm 10.0\%$ – $65.3 \pm 8.6\%$ at every tested concentration.

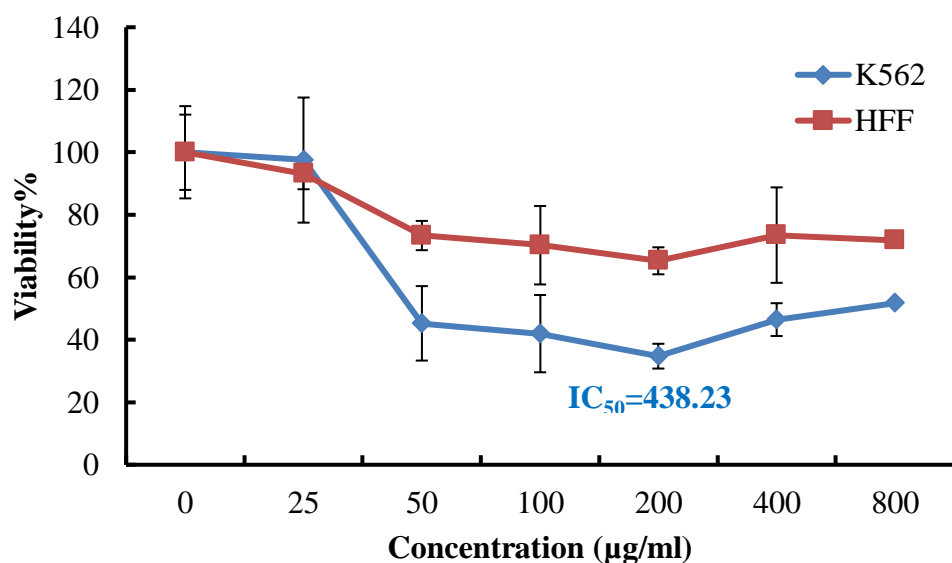





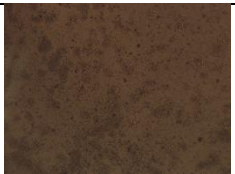




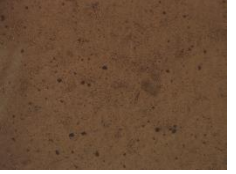


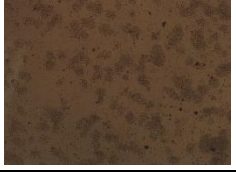
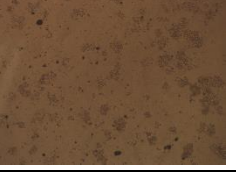



Fig. (7): Cytotoxic effect of ZnO NPs on K562 and HFF cells after 48 hrs incubation at 37 °C.

The assessment shows that CuO NPs are rather three times more cytotoxic to K562 cells in comparison with ZnO NPs, opposing to their IC_{50} values. These findings are consistent with recent research that uncovers that there is higher cytotoxicity of copper-based nanomaterials compared to zinc-based nanomaterials in various cancer cell lines [24,25]. Additional evidence for quantitative results presented in Figure 8 can be found in its micrographs, showing morphological changes in K562 cells with higher CuO NPs concentrations (cell shrinkage and membrane blebbing). The increased toxicity seen in cancer cells should be given special consideration when developing therapeutic strategies. There are several reasonable reasons why the seen selective cytotoxicity occurs. Normal cells are different from cancer cells with

regards to membrane permeability, metabolic rates and antibodies against free radicals which are often distorted in cancer cells [26]. Such qualities can result in increased internalization of nanoparticles and increased sensitivity to oxidative stress. Recent research by [27] demonstrated that copper oxide nanoparticles are selectively accumulated in cancer cells, although they mostly rely on their unique endocytosis function and impaired efflux pathways. The significant variation in cytotoxic effect of CuO and ZnO nanoparticles may largely be attributed to some variance in their physicochemical properties and rate at which they dissolve. The release of Cu ions from CuO NPs is reported to be able to deplete the glutathione levels by a greater amount compared to Zn ions leading to disruption of the redox balance and initialization of the apoptotic pathways specifically in cancer cells [28]. In addition, the quasi-spherical shape of CuO NPs that is presented here could provide easier penetration into cells than Zn. Appearance of protein corona on biosynthesized nanoparticles represents an important interaction affecting overall biological performance of them. The application of biomolecules produced by *L. plantarum* coating to these nanoparticles may regulate how they physically interact with the cells by means of receptor mediated interactions. Protein coronas created out of bacteria may enhance nanoparticle stability and safety, also selectively target and kill cancer cells through their specific molecular recognition [29]. Further investigations are needed to elucidate the cause of the plateau effect in the existence of higher levels of ZnO NPs. Noted similar outcomes when using metal oxide nanoparticles and proposed that agglomeration at high concentrations is the reason behind these limitations due to the decrease in effective surface area and cellular contact [30].

Concentration $\mu\text{g mL}^{-1}$	CuO nanoparticles		ZnO nanoparticles	
	TC ₁	TC ₂	TC ₁	TC ₂
800				
400				
200				
100				




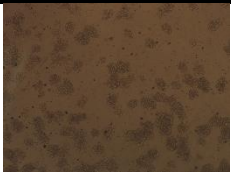
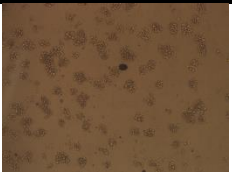




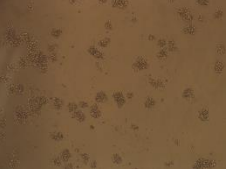




50				
25				
DmsO				

Figure (8): Dose-response curve of K562 erythroleukemic cells cancer cells treated with CuO/ ZnO nanoparticles as determined by MTT assay.

The IC₅₀ values obtained in this study, particularly at 135.46 µg/mL for CuO NPs, are marginal in their potential as a therapeutic advantage. Meta-analyses have reported IC₅₀ values for metal oxide nanoparticles in cancer cell lines covering 25–500 µg/mL range [31,32]. Unlike many old anticancer drugs, these nanoparticles exhibit a specific mechanism of action, which may reduce the unwanted side effects during cancer therapy, even at increased IC₅₀ values.

Conclusion

Lactobacillus plantarum was employed to successfully produce nanoparticle derivatives of CuO and ZnO, demonstrating an environmentally friendly strategy. XRD analysis revealed indications for monoclinic tenorite CuO (24.78 nm) and hexagonal wurtzite ZnO (27.41 nm); while SEM offered images of CuO nanoparticles having quasi-spherical morphologies, and ZnO nanoparticles. The outcome of EDS spectroscopy justified the elemental composition and forward their minimal nature of bacterial residues. The assessment using MTT assay demonstrated great anticancer potency against K562 erythroleukemic cells, where CuO nanoparticles were significantly stronger (IC₅₀ = 135.46 µg/ml) than ZnO (IC₅₀ = 43 Selective cytotoxicity of nanoparticles is evident based on the outcome of toxicity in both cancer and non-cancer cells with HFF fibroblasts maintaining viability above 65% at doses fatal to cancer cells. This preferential cytotoxicity can be accounted for by decreased membrane-stability, deranged metabolic regulation, and lowered antioxidant potential in cancer cells. These results show the promise that biogenically produced metal oxide nanoparticles have to be effective candidates for targeted cancer therapy. The implantation of these nanoparticles into more technologically advanced delivery systems could increase both the therapeutic outcomes of these nanoparticles and their appropriateness for human trials.



References

- [1] Hanahan D, Weinberg RA. Hallmarks of cancer: the next generation. *Cell* 2011;144:646–74.
- [2] Vinardell MP, Mitjans M. Antitumor activities of metal oxide nanoparticles. *Nanomaterials* 2015;5:1004–21.
- [3] Ahamed M, Akhtar MJ, Khan MAM, Alrokayan SA, Alhadlaq HA. Oxidative stress mediated cytotoxicity and apoptosis response of bismuth oxide (Bi₂O₃) nanoparticles in human breast cancer (MCF-7) cells. *Chemosphere* 2019;216:823–31.
- [4] Singh P, Kim Y-J, Zhang D, Yang D-C. Biological synthesis of nanoparticles from plants and microorganisms. *Trends Biotechnol* 2016;34:588–99.
- [5] Khandel P, Yadaw RK, Soni DK, Kanwar L, Shahi SK. Biogenesis of metal nanoparticles and their pharmacological applications: present status and application prospects. *J Nanostructure Chem* 2018;8:217–54.
- [6] Sathiyavimal S, Vasantharaj S, Bharathi D, Saravanan M, Manikandan E, Kumar SS, et al. Biogenesis of copper oxide nanoparticles (CuONPs) using *Sida acuta* and their incorporation over cotton fabrics to prevent the pathogenicity of Gram negative and Gram positive bacteria. *J Photochem Photobiol B* 2018;188:126–34.
- [7] Cuevas R, Durán N, Diez MC, Tortella GR, Rubilar O. Extracellular biosynthesis of copper and copper oxide nanoparticles by *Stereum hirsutum*, a native white-rot fungus from chilean forests. *J Nanomater* 2015;2015:789089.
- [8] Jayaseelan C, Rahuman AA, Kirthi AV, Marimuthu S, Santhoshkumar T, Bagavan A, et al. Novel microbial route to synthesize ZnO nanoparticles using *Aeromonas hydrophila* and their activity against pathogenic bacteria and fungi. *Spectrochim Acta A Mol Biomol Spectrosc* 2012;90:78–84.
- [9] Nicol AW. X-ray Diffraction. *Physicochemical Methods of Mineral Analysis*, Springer; 1975, p. 249–320.
- [10] Patel M, Mishra S, Verma R, Shikha D. Synthesis of ZnO and CuO nanoparticles via Sol gel method and its characterization by using various technique. *Discov Mater* 2022;2:1.
- [11] Sankar R, Maheswari R, Karthik S, Shivashangari KS, Ravikumar V. Anticancer activity of *Ficus religiosa* engineered copper oxide nanoparticles. *Materials Science and Engineering C* 2014;44:234–9. <https://doi.org/10.1016/j.msec.2014.08.030>.
- [12] Akhtar MJ, Ahamed M, Kumar S, Khan MAM, Ahmad J, Alrokayan SA. Zinc oxide nanoparticles selectively induce apoptosis in human cancer cells through reactive oxygen species. *Int J Nanomedicine* 2012:845–57.
- [13] Thatoi P, Kerry RG, Gouda S, Das G, Pramanik K, Thatoi H, et al. Photo-mediated green synthesis of silver and zinc oxide nanoparticles using aqueous extracts of two mangrove plant species, *Heritiera fomes* and *Sonneratia apetala* and investigation of their biomedical applications. *J Photochem Photobiol B* 2016;163:311–8.



-
- [14] Singh M, Goyal M, Devlal K. Size and shape effects on the band gap of semiconductor compound nanomaterials. *Journal of Taibah University for Science* 2018;12:470–5.
- [15] Kiran GS, Dhasayan A, Lipton AN, Selvin J, Arasu MV, Al-Dhabi NA. Melanin-templated rapid synthesis of silver nanostructures. *J Nanobiotechnology* 2014;12:1–13.
- [16] Wang D, Zhao L, Ma H, Zhang H, Guo L-H. Quantitative analysis of reactive oxygen species photogenerated on metal oxide nanoparticles and their bacteria toxicity: the role of superoxide radicals. *Environ Sci Technol* 2017;51:10137–45.
- [17] Raghupathi KR, Koodali RT, Manna AC. Size-dependent bacterial growth inhibition and mechanism of antibacterial activity of zinc oxide nanoparticles. *Langmuir* 2011;27:4020–8.
- [18] Gunalan S, Sivaraj R, Rajendran V. Green synthesized ZnO nanoparticles against bacterial and fungal pathogens. *Progress in Natural Science: Materials International* 2012;22:693–700.
- [19] Jao M-H, Liao H-C, Su W-F. Achieving a high fill factor for organic solar cells. *J Mater Chem A Mater* 2016;4:5784–801.
- [20] Azizi S, Ahmad MB, Namvar F, Mohamad R. Green biosynthesis and characterization of zinc oxide nanoparticles using brown marine macroalga *Sargassum muticum* aqueous extract. *Mater Lett* 2014;116:275–7.
- [21] Gudikandula K, Charya Maringanti S. Synthesis of silver nanoparticles by chemical and biological methods and their antimicrobial properties. *J Exp Nanosci* 2016;11:714–21.
- [22] Sivaraj R, Rahman PKSM, Rajiv P, Narendhran S, Venckatesh R. Biosynthesis and characterization of *Acalypha indica* mediated copper oxide nanoparticles and evaluation of its antimicrobial and anticancer activity. *Spectrochim Acta A Mol Biomol Spectrosc* 2014;129:255–8.
- [23] Kang T, Guan R, Chen X, Song Y, Jiang H, Zhao J. In vitro toxicity of different-sized ZnO nanoparticles in Caco-2 cells. *Nanoscale Res Lett* 2013;8:1–8.
- [24] Islam MJ, Khatun MT, Rahman MR, Alam MM. Green synthesis of copper oxide nanoparticles using *Justicia adhatoda* leaf extract and its application in cotton fibers as antibacterial coatings. *AIP Adv* 2021;11.
- [25] Gudkov S V, Burmistrov DE, Serov DA, Rebezov MB, Semenova AA, Lisitsyn AB. A mini review of antibacterial properties of ZnO nanoparticles. *Front Phys* 2021;9:641481.
- [26] Moloney JN, Cotter TG. ROS signalling in the biology of cancer. *Semin Cell Dev Biol*, vol. 80, Elsevier; 2018, p. 50–64.
- [27] Ghasemi P, Shafiee G, Ziamajidi N, Abbasalipourkabir R. Copper nanoparticles induce apoptosis and oxidative stress in SW480 human colon cancer cell line. *Biol Trace Elem Res* 2023;201:3746–54.
- [28] Khatoon A, Khan F, Ahmad N, Shaikh S, Rizvi SMD, Shakil S, et al. Silver nanoparticles from leaf extract of *Mentha piperita*: eco-friendly synthesis and effect on acetylcholinesterase activity. *Life Sci* 2018;209:430–4.
-



- [29] Payne CK. A protein corona primer for physical chemists. *J Chem Phys* 2019;151.
- [30] Naha PC, Liu Y, Hwang G, Huang Y, Gubara S, Jonnakuti V, et al. Dextran-coated iron oxide nanoparticles as biomimetic catalysts for localized and pH-activated biofilm disruption. *ACS Nano* 2019;13:4960–71.
- [31] Jayarambabu N, Akshaykranth A, Rao TV, Rao KV, Kumar RR. Green synthesis of Cu nanoparticles using *Curcuma longa* extract and their application in antimicrobial activity. *Mater Lett* 2020;259:126813.
- [32] Prabhu YT, Rao KV, Kumari BS, Kumar VSS, Pavani T. Synthesis of Fe_3O_4 nanoparticles and its antibacterial application. *Int Nano Lett* 2015;5:85–92.

